ACS APPLIED MATERIALS & INTERFACES

Research Article

www.acsami.org

Organic One-Transistor-Type Nonvolatile Memory Gated with Thin Ionic Liquid-Polymer Film for Low Voltage Operation

Sun Kak Hwang, Tae Joon Park, Kang Lib Kim, Suk Man Cho, Beom Jin Jeong, and Cheolmin Park*

Department of Materials Science and Engineering, Yonsei University, 134 Shinchon-dong, Seodaemoon-gu, Seoul 120749, Republic of Korea

Supporting Information

ABSTRACT: As one of the most emerging next-generation nonvolatile memories, one-transistor (1T)-type nonvolatile memories are of great attention due to their excellent memory performance and simple device architecture suitable for high density memory arrays. In particular, organic 1T-type memories containing both organic semiconductors and insulators are further beneficial because of their mechanical flexibility with low cost fabrication. Here, we demonstrate a new flexible organic 1T-type memory operating at low voltage. The low voltage operation of a memory less than 10 V was obtained by employing a polymer gate insulator solution blended with ionic liquid as a charge storage layer. Ionic liquid homogeneously dissolved in a thin poly(vinylidene fluoride-*co*-trifluoroethylene) (PVDF-TrFE) film gave rise to low voltage operation of a device due to its high capacitance. Simultaneously, stable charge trapping of either anions or cations efficiently occurred in the polymer matrix, dependent upon gate bias. Optimization of ionic liquid in PVDF-TrFE thus led to an air-stable and mechanically flexible organic 1T-type nonvolatile memory operating at programming voltage of ±7 V with large ON/OFF current margin of approximately 10^3, reliable time-dependent data retention of more than 10^4 seconds, and write/read endurance cycles of 80.

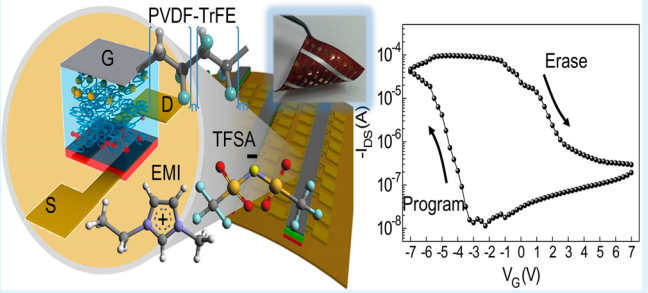

KEYWORDS: *organic memory, field effect transistor memory, ionic liquid-polymer gate insulators, low voltage operation, charge trapping memory, flexible memory*

1. INTRODUCTION

One-transistor (1T)-type nonvolatile memories, based on nondestructive bistable electrical conductance of semiconductor channel gated by functional insulators, are of great interest due to their excellent memory performance and very simple device architecture suitable for high density memory arrays. The 1T-type nonvolatile memories can be categorized in terms of the origin of bistable semiconducting channel conductance into charge trapping memories[1] and ferroelectric ones,[2] with at least two different levels of gate-programmed charge storage and spontaneous polarization, respectively. Various novel materials have been developed for high performance 1T-type memory including ferroelectrics,[2,3] charge trapping[4−7] and blocking layers,[8−11] electrodes,[12] and semiconductors.[13−19] As a result, the memory performance was significantly improved such as endurance,[20,21] data retention,[3,10,21,22] program speed,[22,23] flexibility,[24−26] printing capability,[27] ON/OFF memory margin,[20,28] and operating voltage,[8,29] making these types of memories competitive with conventional floating gate ones. Moreover, the organic 1T-type memories containing both organic semiconductors and insulators offer additional benefits of low cost, easy fabrication, and mechanical flexibility in particular when these layers are solution-processed.

Among technological issues that still limit the utilization of the memory, high voltage operation of an organic 1T memory is one of the most serious obstacles which should be overcome with a top priority. In fact, most organic 1T memory devices need a gate voltage, often ranging from ±13 to over 200 V due to the use of thick ferroelectric or charge trapping and blocking layers to reduce the leakage current resulting from numerous structural defects, including pinholes, residual solvent, and grain boundaries.[1,2] Several 1T-type nonvolatile memories operated below ±10 V have recently been demonstrated. The key materials for the low voltage operation were, however, based on either vacuum deposited organic or inorganic oxide semiconductors[17,30] with organic/inorganic hybrid insulating layers such as AlO_x,[6−8,14] TiO_x,[10] and organosilicate,[31] making it difficult for these approaches to be cost-effective and more importantly mechanically flexible. We envisioned that high capacitance ionic liquids, which have been widely employed to organic field effect transistors (OTFTs) for low voltage operation,[32−34] can be also suitable for 1T type nonvolatile memory as long as gate-field dependent bistable conductance is guaranteed with reliable time-dependent data retention and read−write cycle endurance.

Received: August 25, 2014
Accepted: October 24, 2014
Published: October 24, 2014

   dx.doi.org/10.1021/am505750v | *ACS Appl. Mater. Interfaces* 2014, 6, 20179−20187

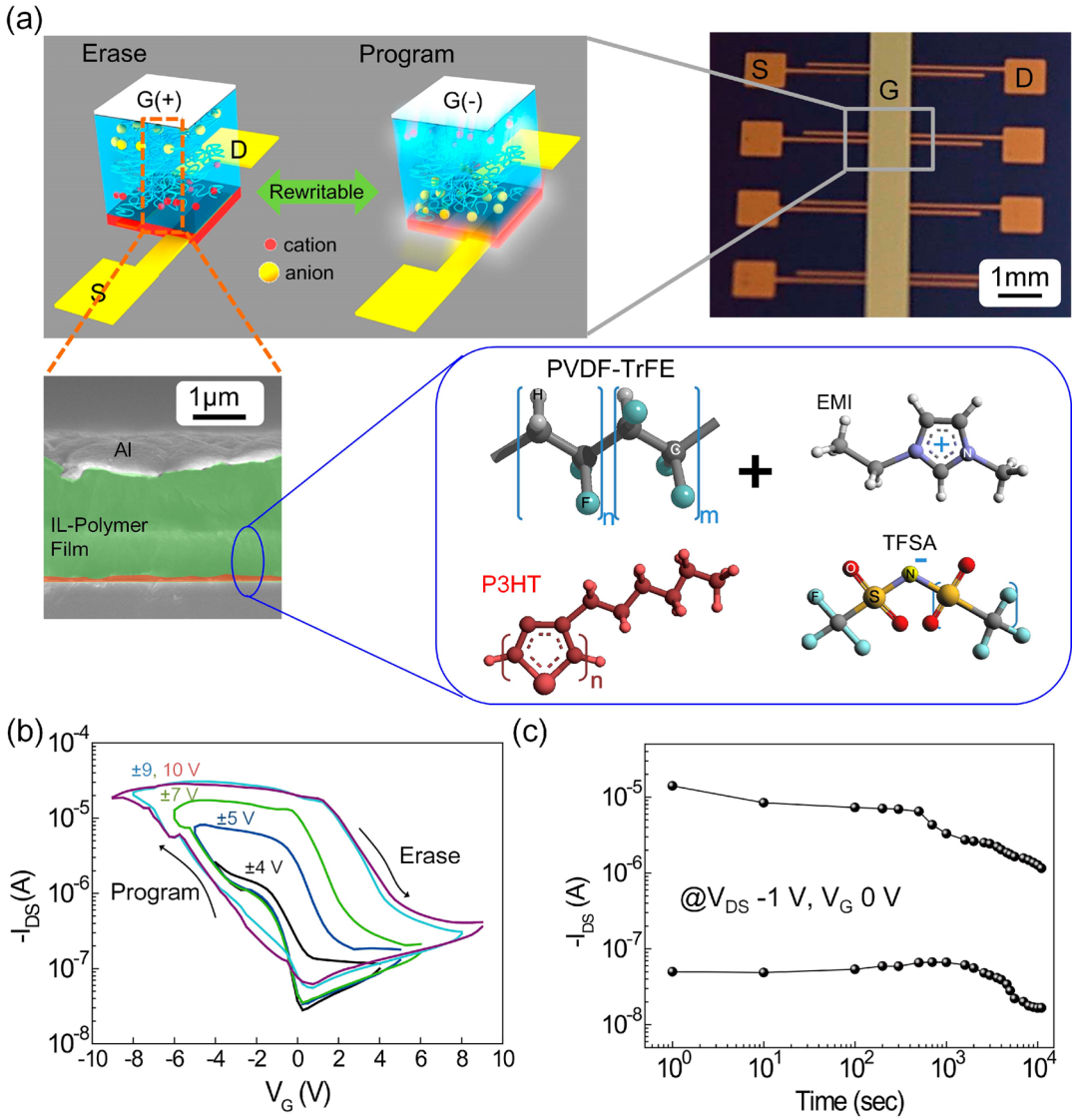

Figure 1. (a) Schematics illustrating the operation of an organic 1T-type nonvolatile memory with a P3HT channel and an EMI[TFSA]-PVDF-TrFE insulator film. Photograph (right) and SEM image (left) of the plan and cross-sectional views of a 1T-type memory device, respectively, are also shown with the chemical structure of P3HT, EMI[TFSA], and PVDF-TrFE. (b) I_{DS}–V_G transfer curves of a device containing an IL-polymer film with 10 wt % EMI[TFSA] concentration. The current hysteresis arises from the nonvolatile charge storage of the IL-polymer film. (c) The time-dependent retention characteristics of I_{DS} values established in the 1T-type memory device. The ON and OFF states were programmed or erased at V_G of ±7 V.

Here, we present a highly reliable and flexible organic 1T-type memory with low voltage operation. A memory operating at voltage of less than 10 V was obtained by employing a polymer gate insulator solution-blended with ionic liquid (IL) as a charge storage layer. IL homogeneously dissolved in a thin poly(vinylidene fluoride-*co*-trifluoroethylene) (PVDF-TrFE) film allowed for the low voltage operation of a device due to its high capacitance. Simultaneously, stable charge trapping of either anions or cations efficiently occurred in the polymer matrix, dependent upon gate bias. Optimization of IL in PVDF-TrFE thus led to an air-stable and mechanically flexible organic 1T-type nonvolatile memory operating at programming voltage of ±7 V with large ON/OFF current margin of approximately 10^3, reliable time-dependent data retention of more than 10^4 seconds and write–read endurance cycles of 80.

2. EXPERIMENTAL SECTION

Materials and Film Preparation. PVDF-TrFE with 25 wt % TrFE (MSI Sensors), poly(3-hexylthiophene) (P3HT) (Sigma-Aldrich, Korea), and poly(vinylidene fluoride-*co*-hexafluoropropylene) (PVDF-HFP) (Sigma-Aldrich, Korea) were used without further purification. P3HT has weight-average molecular weight (M_w) of 180 000 g mol^{-1} with 98.5% head to tail regioregularity.[24] Samsung Electronics Co. Ltd. kindly provided poly(vinylidene-fluoride–trifluoroethylene–chlorotrifluoroethylene) (PVDF-TrFE-CTFE) with its monomer ratio of 66:34:8.3. 1-Ethyl-3-methylimidazolium bis-(trifluoromethylsulfonyl) amide (EMI[TFSA]) (Tokyo Chemical Industry Co) and organic solvents including methyl ethyl ketone (MEK), acetone, and chloroform (Sigma-Aldrich, Korea) were used as received. A P3HT solution in chloroform (1 wt %) was spin-coated at 2000 rpm for 60 s on prepatterned Au S/D electrodes thermally deposited on either a Si/SiO_2 (200 nm) or a polyimide substrate. The IL-polymer solutions were prepared by codissolving polymers and EMI[TFSA] in MEK and spin-coated at 1500 rpm for 60 s on a P3HT layer. For IL-PVDF-TrFE films, the concentration of PVDF-TrFE was

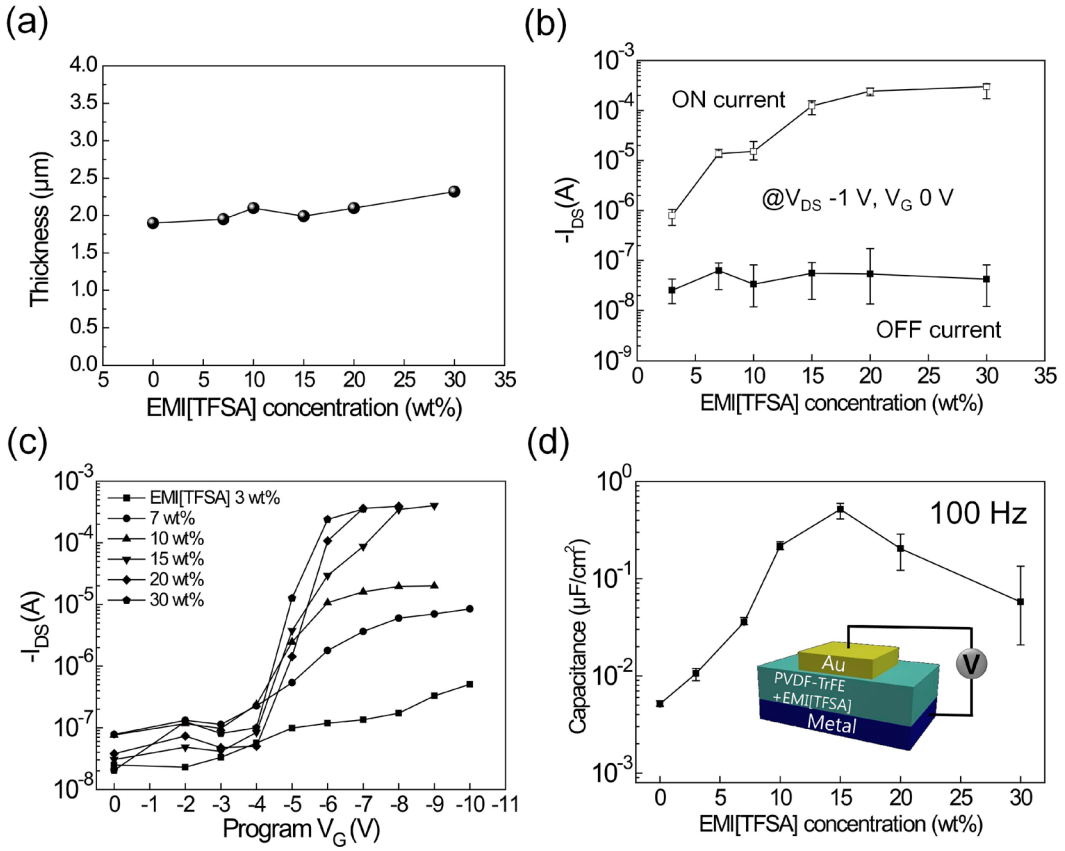

Figure 2. (a) Thickness of IL-polymer films as a function of EMI[TFSA] concentrations with respect to PVDF-TrFE. (b) ON and OFF current values of 1T-type memories with various IL-polymer insulators. The read voltage (V_G) was 0 V. The sets of more than 5 cells were used to obtain the distribution of both ON/OFF current values. (c) I_{DS} values of 1T-type memory devices with IL-polymer insulators obtained at a read voltage after various program V_G in the dc sweep mode. (d) Specific capacitance from capacitance−voltage measurements at $V = 0$ of Au/IL-polymer film/highly doped Si capacitors as a function of IL concentrations.

maintained at 10 wt % in solvent, while the IL concentration was varied from 3, 5, 7, 10, 15, 20, and 30 wt % with respect to PVDF-TrFE.

Capacitor Fabrication and Characterization. Highly doped Si/IL-polymer films/metal capacitors were fabricated as described in our previous works.[24] Patterned Au top electrodes were thermally evaporated on IL-polymer films using a shadow mask (SNTEK MEP5000). $C-V$ characteristic was measured at a frequency of 100 Hz under ambient conditions (Agilent 4284A precision LCR meter). The thickness of IL-polymer films was evaluated using an Alpha step 500 surface profiler (AS500) (KLA-Tencor Co.).

Fabrication and Characterization of 1T-Type Memory. Top-gate-bottom-contact polymer memories were fabricated similarly to our previous devices with ferroelectric polymers.[24,29] On the patterned 30 nm thick Au S/D electrodes thermally evaporated on a substrate, an approximately 50 nm thick P3HT layer and a thin film formation of an IL-polymer insulator were sequentially spin-coated. The PVDF-TrFE/ionic liquid solution in MEK rarely affected the P3HT layer. After removal of the residual solvent by thermal treatment at 60 °C for 2 h, arrays of 70 nm thick top gate Al electrodes were thermally deposited. Oxygen plasma produced by reactive ion etching (RIE) (Femto VITA-4E) was treated to make the Au S/D electrodes accessible with contact probe tips, giving rise to top-gate bottom-contact polymer memories, as illustrated in the schematic in Figure 1a. The electrical properties of devices were examined by characterization systems (ES270B, Agilent Technologies, 2636A, Keithley Instruments Inc.) in ambient conditions. The dynamic characteristics were measured using a Keithley 4200-SCS semiconductor parameter analyzer.

Structure Characterization. The molecular and microstructures of the films were examined using optical microscope (OM) (Olympus BX 51M), field emission scanning electron microscopy (FESEM, LEO 1550 VP), tapping mode atomic force microscopy (TM-AFM, Nanoscope IV a Digital Instruments), and two-dimensional (2D) grazing-incidence wide-angle X-ray scattering (GIWAXS) as described in detail in our previous works.[24,29]

3. RESULTS AND DISCUSSION

Arrays of organic 1T-type memory devices with top-gate bottom-contact structure consisting of polymeric semiconductor and charge trap-detrap layer were constructed on a Si/SiO_2 wafer or a flexible substrate as shown in Figure 1a. Cross-section of an organic 1T-type memory device was also visualized in Figure 1a. Our organic 1T-type memory showed p-type output characteristics in the source-drain current (I_{DS}) versus source-drain voltage (V_{DS}) curve as expected (Supporting Information, Figure S1). Hysteresis loop as a function of a gate voltage (V_G) was observed in the transfer characteristics (at a V_{DS} of −1 V), as shown in Figure 1b. The I_{DS} hysteresis curves were progressively developed with gate voltage sweep and fully saturated at the voltage sweep less than ±10 V as shown in Figure 1b. Furthermore, the bistable ON and OFF current values were retained for more than 10^4 seconds, as shown in Figure 1c. Our results are promising when compared with recent state-of-the art research in which the organic 1T-type polymer memory with vacuum deposited semiconductor operated at ±13 V.[35] Furthermore, the memory performance of our organic 1T device is very comparable with that of a device containing inorganic dielectric layer and/or semiconductor, as shown Supporting Information, Table 1.

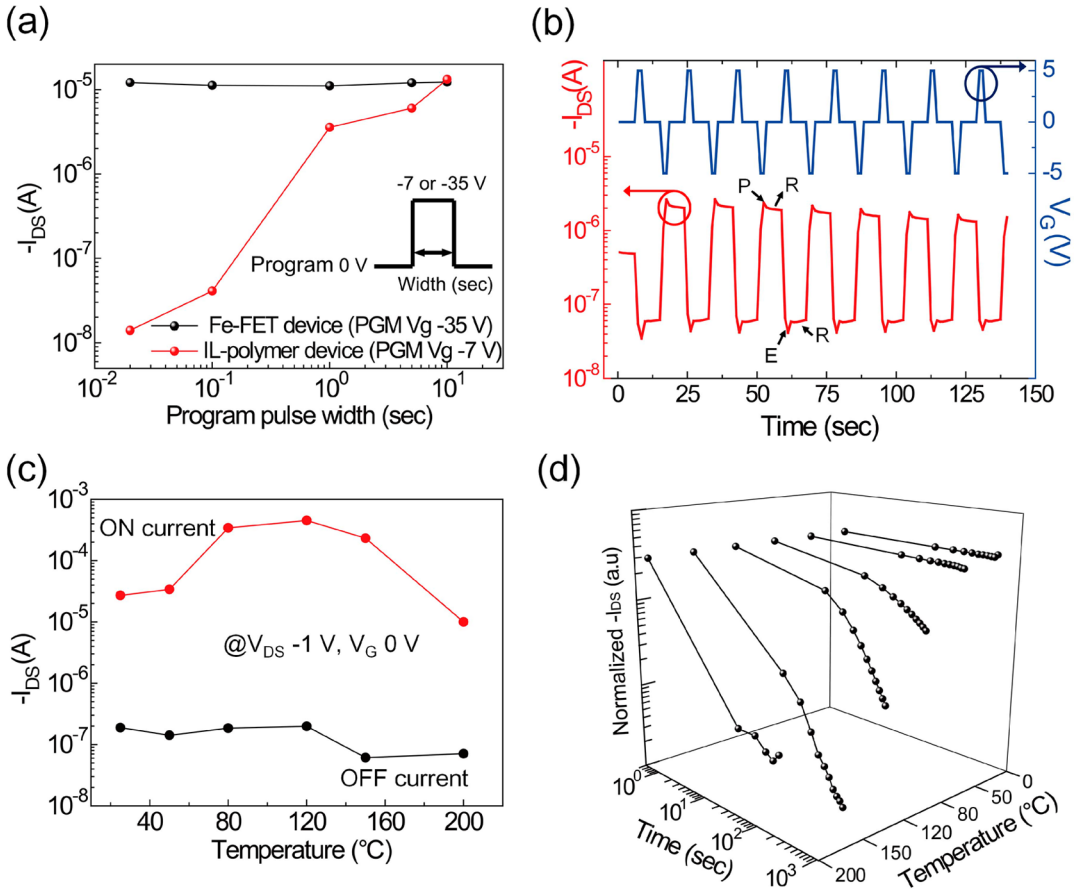

Figure 3. (a) Switching behaviors from OFF to ON state of a ferroelectric 1T memory with a pure PVDF-TrFE insulator and an organic 1T memory containing an IL-polymer film with 10 wt % EMI[TFSA] concentration with respect to PVDF-TrFE as a function of the width of pulsed voltage train. Voltage pulses of −7 and −35 V were programmed to the gate for the organic and ferroelectric 1T memory devices, respectively. While the ferroelectric memory was turned on even with 10^{-2} second pulse, the organic 1T memory was switched after 1 s pulse. (b) I_{DS} dynamics with V_G sequence program (P)-read (R)-erase (E)-read (R) (±5 V, 1 s pulse width) at V_{DS} = −1 V. (c) The ON and OFF current values of an organic 1T device with IL-polymer film having 10 wt % EMI[TFSA] concentration as a function of temperature. (d) Normalized ON current data retention with respect to time of an organic 1T-type memory examined at various temperatures.

We hypothesized that the hysteresis was attributed to the gate voltage dependent bistable storage of ions at the interface between IL-polymer insulator and P3HT. After a large negative V_G of more than −4 V is applied, the anions, which have been homogeneously dissolved throughout polymer matrix, start to move into the interface, resulting in a rapid increase of the I_{DS} owing to hole accumulation in the P3HT channel as shown in Figure 1a. When the V_G returned to zero, the I_{DS} still remained high because of anions physically trapped at the interface. Positive V_G subsequently applied to the device gradually detraps anions and at the same time began to trap cations at the interface, leading to a rapid decrease of I_{DS}. Again, when the V_G became zero, the I_{DS} remained low due to the trapped cations at the interface.

We investigated the memory performance of the devices as a function of the amounts of IL. The IL-polymer films with different EMI[TFSA] compositions showed the similar thickness of approximately 2 μm, as shown in Figure 2a. Apparently, ON current increased with increasing IL due to the increase of interfacial charge density as shown in Figure 2b (Supporting Information, Figure S2a). The gate leakage current of an IL-polymer film increased with IL concentrations due to facile formation of continuous ion channels through the film with IL (Supporting Information, Figure S2b). The gate leakage level of our device with a 10 wt % IL-polymer film is comparable with that of the previous ion-gel gated transistor.[36] As shown in the results of current variation as a function of sweep program voltage in Figure 2c, current hysteresis is fully saturated below 10 V of a device containing EMI[TFSA] more than 7 wt % with respect to PVDF-TrFE. On the other hand, a device with a neat PVDF-TrFE insulator showed a saturated I_{DS} hysteresis with a gate voltage sweep above ±100 V due to the large coercive field of a PVDF-TrFE for ferroelectric polarization switching (50 MV/m) (Supporting Information, Figure S2d).

The capacitance−voltage (C−V) and capacitance−frequency characteristics were examined from Au/IL-polymer films/highly doped Si capacitors with different IL compositions. When the forward and backward bias was swept from −2 to +2 V, the capacitors showed typical C−V curves (Supporting Information, Figure S3a),[37] and the specific capacitances of the IL-polymer films were obtained at 0 V. Ionic-liquid films largely decrease at high frequency due to slow motion of ions as shown in Supporting Information, Figure S3b. The measured maximum capacitances at 100 Hz are approximately ∼1 μF cm^{-2}, while a pure PVDF-TrFE shows a specific capacitance value of ∼30 nF cm^{-2}, as shown in Figure 2d. The large capacitance values of the IL-polymer films are attributed to the electrical double layers at the interface between the electrodes

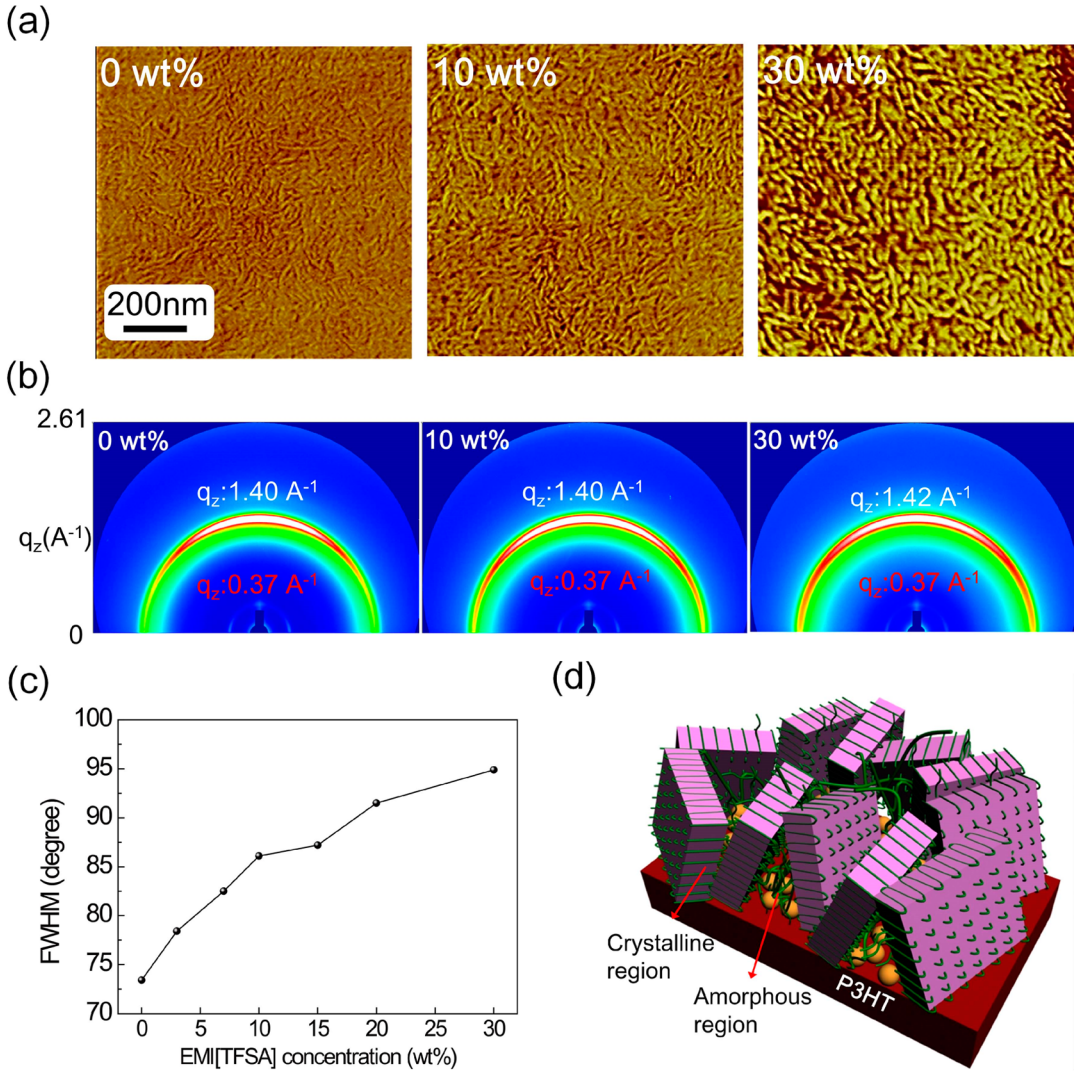

Figure 4. (a) TM-AFM images in height mode and (b) GIWAXS patterns of the IL-polymer films on P3HT layer as a function of EMI[TFSA] concentration with respect to polymer. (c) fwhm values of equatorial azimuthal intensity profiles of q_z = (110) and/or (200) peaks as a function of EMI[TFSA] concentratons. (d) A schematic illustration of microstructure of the IL-polymer film in which ions were preferentially dissolved in the amorphous regions of semicrystalline PVDF-TrFE matrix.

and ionic liquids. In fact, the capacitances of our thin solid IL-polymer films can further increase with IL and become comparable with those of ion gels reported previously.[36,38] The amount should be, however, optimized for reliable memory performance. For instance, in spite of the square-like current hysteresis with a large ON/OFF ratio in a device containing 30 wt % IL, ON current data retention with time was poor with significant drop of an initial current level within 500 s (Supporting Information, Figure S2c). Anions could be easily detrapped at the interface due to their strong interaction with nearby cations abundant in such a high concentration of IL. It should be also noted that the equivalent PVDF-TrFE thickness of our IL-polymer film with 10 wt % EMI[TFSA] concentration calculated at 100 Hz is approximately 50 nm which is thin enough for device operation below 10 V. Our IL-polymer film with bistable charge storage capability as well as high capacitance gave rise to novel organic 1T-type memory with low voltage operation.

To further reveal the operation mechanism of our memory, we investigated its switching behavior in comparison with a conventional ferroelectric 1T memory with a pure PVDF-TrFE insulator whose switching time was approximately 10^{-3} to 10^{-4} seconds.[22] Furthermore, the dynamic switching response of a device was measured as a function of pulse widths. Switching between program and erase states occurred upon the application of gate voltage pulses with the drain voltage at −1 V. The memory margin of current ON/OFF ratio of approximately 10^2 was maintained during the dynamic switching with 1 s pulse width. As shown in Figure 3a,b and Supporting Information, Figure S4a−c, our devices require switching times longer than 1 s due to rather slow ionic motion.[39] One possible way to reduce switching time of our device would be to employ a high k polymer matrix whose strong polarization can make anion−cation pairs readily dissociated, leading to the enhancement of ion mobility.[40] For instance, a poly(vinylidenefluoride−trifluoroethylene−chlorofloroethylene) can be a good candidate for the purpose with its dielectric constant of approximately 60.[41] We also examined current hysteresis and time-dependent retention behavior of a device as a function of temperature as shown in Figure 3c,d, respectively (also see Supporting Information, Figure S4d). The device showed the good bistable current

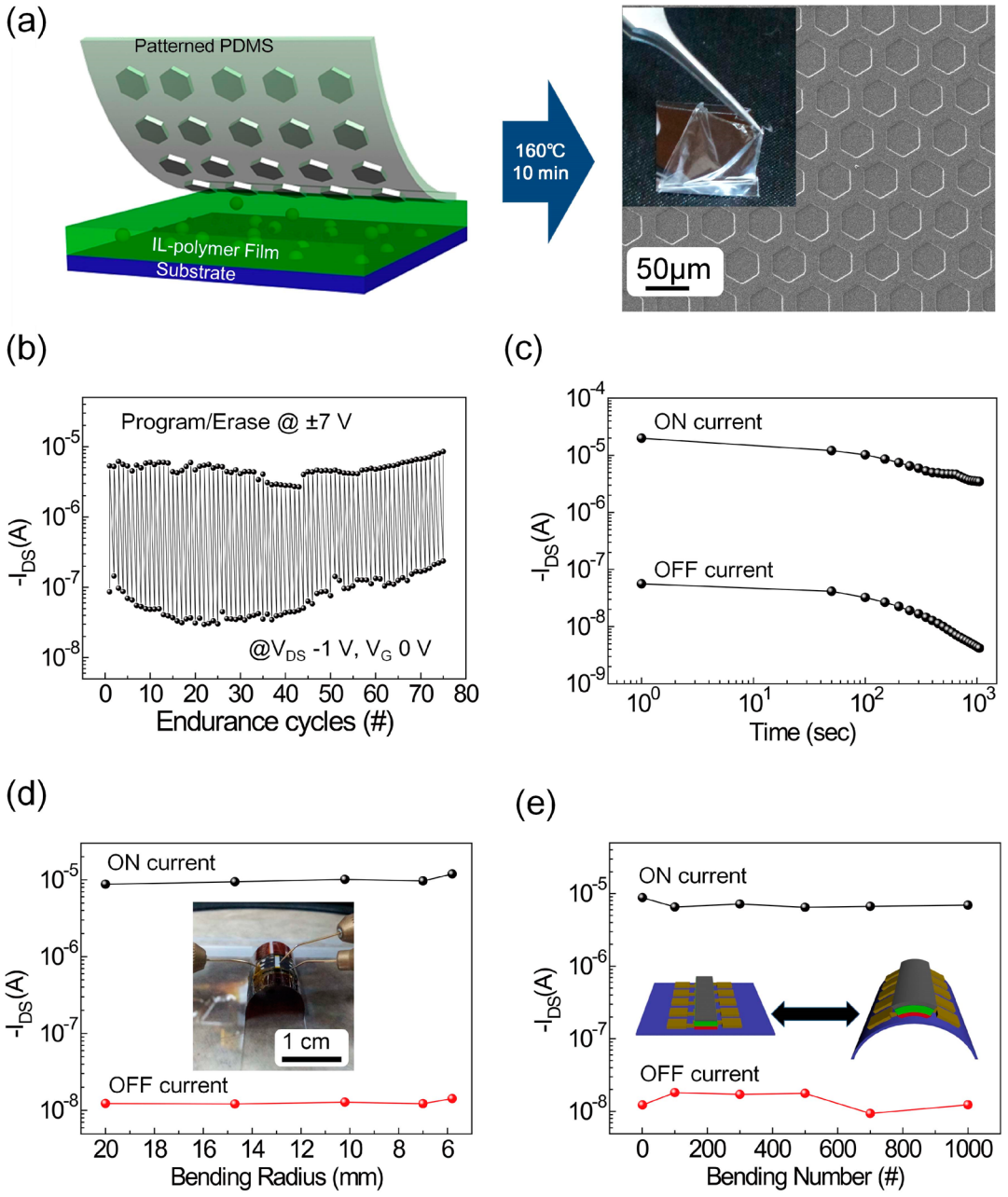

Figure 5. (a) Schematic of the fabrication of a micropatterned IL-polymer film by microimprinting. SEM image of a topographically patterned EMI[TFSA]/PVDF-TrFE (10/90) film after thermal imprinting with a prepatterned PDMS mold consisting of 30 μm hexagons in size. The inset shows a photograph of a micron-thick free-standing solid IL-polymer film. The write/erase endurance cycles (b) and time-dependent retention characteristics (c) of bistable I_{DS} values of an organic 1T-type memory fabricated on a polyimide substrate. The I_{DS} values of a flexible organic 1T-type memory as a function of (d) the bending radius and (e) the number of bending cycles at a bending radius of 5.8 mm. The inset in part d is a photograph of a flexible organic IL-polymer memory *in situ* measured under bending.

behavior at temperatures up to 150 °C which is well above the Curie temperature of PVDF-TrFE (T_c = 120 °C). In general, the pure PVDF-TrFE behaves as a dielectric with high polarization above the Curie temperature. As the temperature increased to 120 °C, the ON current data retention gradually degraded because of lower activation energy for ionic transport in PVDF-TrFE matrix, and ill-defined hysteresis curve was obtained at 200 °C due to melting of PVDF-TrFE (Figure 3d). It should be, however, noted that our memory has thermal operation margin up to at least 70 °C. Not surprisingly, our organic 1T-type IL-polymer memory devices were also successfully fabricated with other nonferroelectric polymers such as PVDF-HFP and PVDF-TrFE-CTFE, making our method universal (Supporting Information, Figure S5). The results in Figure 3 support the ion trapping and detrapping principle of our device.

The molecular and microstructures of the IL-polymer films on P3HT surface were visualized by TM-AFM and 2D GIWAXS. All IL-polymer films with various IL concentrations exhibited the characteristic PVDF-TrFE crystalline structures with randomly distributed needle-like microdomains, and representative surface morphologies are shown in Figure 4a (also see Supporting Information, Figure S6a). The microdomains of PVDF-TrFE increased in size with EMI[TFSA]

concentration due to the solvating effect of IL on polymer crystallization (Supporting Information, Figure S6a). The root-mean-square (RMS) roughness of IL-polymer films was also measured using AFM, as plotted Supporting Information, Figure S6b. The RMS of active layer, P3HT, is approximately 0.691 nm. The roughness of dielectric layer did not change significantly with IL concentrations but abruptly increased at high IL concentration over 20 wt %. It should be noted that a 10 wt % IL-polymer film we used for memory device has its roughness similar to that of a neat PVDF-TrFE film. The 2D GIWAXS patterns of IL-polymer films on P3HT are shown in Figure 4b and Supporting Information, Figure S7. These patterns display a reflection at a scattering vector, q_z, of approximately 1.40−1.41 Å^{-1} preferentially intensified at the meridian, arising from (110) or (200) plane of the PVDF-TrFE crystals.[42,43] The diffraction patterns also show multiple reflections at q_z of approximately 0.37 Å^{-1} corresponding to the (100) plane of P3HT crystals.[44] The results apparently indicate that both PVDF-TrFE and P3HT have their chains aligned parallel to the surface. Moreover, as the amount of EMI[TFSA] increased, the full width half-maximum (fwhm) of the azimuthal angle intensity of q_z, (110) or (200) peaks, increased as shown in Figure 4c, which implies that the preferred orientation of the PVDF-TrFE crystals was slightly destroyed with IL. The molecular and microstructures of IL-polymer insulators in conjuction with both switching and temperature dependent memory performance clearly suggest that anions and cations were properly trapped and detrapped, dependent upon gate bias, in the amorphous regions of PVDF-TrFE near the interface with P3HT as shown in the scheme of Figure 4d. It should be noted that various structural properties (e.g., chemical structure, vacancy, aggregate, solvent residue, and etc.) of polymer films can also play a role in charge trapping−detrapping behaviors, thus memory effects in transistors. Furthermore, the role of the interface between semiconducting and dielectric layer is of prime importance in our memory device. We believe that ions are preferentially trapped and detrapped at the interfacial regions. In addition, on the basis of the previous work in which PVDF crystals were not damaged with ionic liquid,[36] we assume that the ions were preferentially located in the amorphous regions of PVDF-TrFE at the interface with P3HT.

Our thin solid IL-polymer films with good thermal stability are conveniently combined with direct thermoimprinting for fabricating micropatterns, and the results are shown in Figure 5a. An IL-polymer film was compressed at 160 °C and the low pressure of 5 kPa with a prepatterned poly(dimethylsiloxane) elastomeric (PDMS) mold as shown in the scheme of Figure 5a. A topographic microstructure with periodic hexagonal holes was readily developed over the large area. Furthermore, a mechanically flexible organic 1T-type memory was successfully fabricated on a conventional polyimide substrate. The device programmed at ±7 V again shows reliable nonvolatile memory performance comparable with that on Si/SiO_2, as shown in Figure 5b,c. However, as shown in Figure 5b, the OFF current tends to increase with write−erase cycle numbers possibly due to the increase of the deeply trapped anions IL into the P3HT with cycles. A charge blocking layer can be considered to resolve the issue. The ON and OFF current values at a read voltage of −1 V were rarely fluctuated under various *in situ* bending conditions with the lowest bending radius of 5.8 mm, as shown in Figure 5d (Supporting Information, Figure S8a). Figure 5e shows that ON and OFF current margin of the device was not significantly altered even after more than 1000 bending cycles at a radius of 5.8 mm (Supporting Information, Figure S8b). Beneficially, our organic 1T type memory was also extremely air-stable, and thus, its performance was maintained even after air-exposure of a device for 2 months without significant degradation (Supporting Information, Figure S9).

4. CONCLUSIONS

In summary, we demonstrated organic 1T-type nonvolatile memory operating at low voltage of ±7 V with excellent data reliability. The performance was attributed to our novel charge storage layers of IL-polymer films prepared by solution-blending of insulating polymers and ionic liquids. The EMI[TFSA] in the film significantly reduced the operating voltage due to its high capacitance. More importantly, ions accumulated and physically trapped in the amorphous regions of PVDF-TrFE near the interface with semiconductor gave rise to good data reliability. Thin solid IL-polymer films with both mechanical and thermal stability allowed for a flexible memory that exhibited ON/OFF current ratio of 10^3, data retention of approximately 10^4 seconds and read and write cycle endurance of 80. Furthermore, the device was tolerant upon more than 1000 bending cycles at a bending radius of 5.8 mm. Our results clearly indicate that the developed flexible, air-stable nonvolatile polymer memory even without elaborately designed charge control layers can be readily combined with other emerging mobile organic electronic devices.

■ ASSOCIATED CONTENT

Supporting Information

AFM images, GIWAX data, MFM, and *I*−*V* characteristics results. This material is available free of charge via the Internet at http://pubs.acs.org/.

■ AUTHOR INFORMATION

Corresponding Author

*Phone: 82-2-2123-2833. Fax: 82-2-312-5375. E-mail: cmpark@yonsei.ac.kr.

Notes

The authors declare no competing financial interest.

■ ACKNOWLEDGMENTS

This research was supported by Samsung Research Funding Center of Samsung Electronics under Project SRFC-MA1301-03.

■ REFERENCES

(1) Han, S.-T.; Zhou, Y.; Roy, V. A. L. Towards the Development of Flexible Non-Volatile Memories. *Adv. Mater.* **2013**, *25*, 5425−5449.

(2) Park, Y. J.; Bae, I.; Kang, S. J.; Chang, J.; Park, C. Control of Thin Ferroelectric Polymer Films for Non-Volatile Memory Applications. *IEEE Trans. Dielectr. Electr. Insul.* **2010**, *17*, 1135−1163.

(3) Kim, R. H.; Kim, H. J.; Bae, I.; Hwang, S. K.; Velusamy, D. B.; Cho, S. M.; Takaishi, K.; Muto, T.; Hashizume, D.; Uchiyama, M.; Andre, P.; Mathevet, F.; Heinrich, B.; Aoyama, T.; Kim, D.-E.; Lee, H.; Ribierre, J.-C.; Park, C. Non-Volatile Organic Memory with Sub-Millimetre Bending Radius. *Nat. Commun.* **2014**, *5*, 3583.

(4) Rani, A.; Song, J.-M.; Lee, M. J.; Lee, J.-S. Reduced Graphene Oxide Based Flexible Organic Charge Trap Memory Devices. *Appl. Phys. Lett.* **2012**, *101*, 233308.

(5) Kim, Y.-H.; Kim, M.; Oh, S.; Jung, H.; Kim, Y.; Yoon, T.-S.; Kim, Y.-S.; Lee, H. H. Organic Memory Device with Polyaniline Nanoparticles Embedded as Charging Elements. *Appl. Phys. Lett.* **2012**, *100*, 163301.

(6) Tsai, T.-D.; Chang, J.-W.; Wen, T.-C.; Guo, T.-F. Manipulating the Hysteresis in Poly(vinyl alcohol)-Dielectric Organic Field-Effect Transistors Toward Memory Elements. *Adv. Funct. Mater.* **2013**, *23*, 4206−4214.
(7) Cho, B.; Kim, K.; Chen, C.-L.; Shen, A. M.; Truong, Q.; Chen, Y. Nonvolatile Analog Memory Transistor Based on Carbon Nanotubes and C60 Molecules. *Small* **2013**, *9*, 2283−2287.
(8) Kim, B. J.; Ko, Y.; Cho, J. H.; Cho, J. Organic Field-Effect Transistor Memory Devices Using Discrete Ferritin Nanoparticle-Based Gate Dielectrics. *Small* **2013**, *9*, 3784−3791.
(9) Zhou, Y.; Han, S.-T.; Xu, Z.-X.; Roy, V. A. L. *Nanoscale* **2013**, *5*, 1972−1979.
(10) Xia, G.; Wang, S.; Zhao, X.; Zhou, L. High-Performance Low-Voltage Organic Transistor Memories with Room-Temperature Solution-Processed Hybrid Nanolayer Dielectrics. *J. Mater. Chem. C* **2013**, *1*, 3291−3296.
(11) Lee, S.; Lee, J.; Lee, H.; Yuk, Y. J.; Kim, M.; Moon, H.; Seo, J.; Park, Y.; Park, J. Y.; Ko, S. H.; Yoo, S. Overcoming the "Retention vs. Voltage" Trade-Off in Nonvolatile Organic Memory: Ag Nanoparticles Covered with Dipolar Self-Assembled Monolayers as Robust Charge Storage Nodes. *Org. Electron.* **2013**, *14*, 3260−3266.
(12) Kang, M.; Baeg, K.-J.; Kim, D.; Noh, Y.-Y; Kim, D.-Y. Printed, Flexible, Organic Nano-Floating-Gate Memory: Effects of Metal Nanoparticles and Blocking Dielectrics on Memory Characteristics. *Adv. Mater.* **2013**, *23*, 3503−3512.
(13) Leong, W. L.; Mathews, N.; Tan, B.; Vaidyanathan, S.; Dotz, F.; Mhaisalkar, S. Solution Processed Non-Volatile Top-Gate Polymer Field-Effect Transistors. *J. Mater. Chem.* **2011**, *21*, 8971−8974.
(14) Yu, W. J.; Chae, S. H.; Lee, S. Y.; Duong, D. L.; Lee, Y. H. Ultra-Transparent, Flexible Single-Walled Carbon Nanotube Non-Volatile Memory Device with an Oxygen-Decorated Graphene Electrode. *Adv. Mater.* **2011**, *23*, 1889−1893.
(15) Bertolazzi, S.; Krasnozhon, D.; Kis, A. Nonvolatile Memory Cells Based on MoS_2/Graphene Heterostructures. *ACS Nano* **2013**, *7*, 3246−3252.
(16) Chiu, Y.-C.; Liu, C.-L.; Lee, W.-Y.; Chen, Y.; Kakuchi, T.; Chen, W.-C. Multilevel Nonvolatile Transistor Memories using a Star-Shaped Poly((4-diphenylamino)benzyl methacrylate) Gate Electret. *NPG Asia Mater.* **2013**, *5*, e35.
(17) Lee, G.-G.; Tokumitsu, E.; Yoon, S.-M.; Fujisaki, Y.; Yoon, J.-W. The Flexible Non-Volatile Memory Devices using Oxide Semiconductors and Ferroelectric Polymer Poly(vinylidene fluoride-trifluoroethylene). *Appl. Phys. Lett.* **2011**, *99*, 012901.
(18) Kang, S. J.; Bae, I.; Park, Y. J.; Park, T. H.; Sung, J.; Yoon, S. C.; Kim, K. H.; Choi, D. H.; Park, C. Non-Volatile Ferroelectric Poly(vinylidene fluoride-*co*-trifluoroethylene) Memory Based on a Single-Crystalline Tri-isopropylsilylethynyl Pentacene Field-Effect Transistor. *Adv. Funct. Mater.* **2009**, *19*, 1609−1616.
(19) Naber, R. C. G.; De Boer, B.; Blom, P. W. M.; De Leeuw, D. M. Low-Voltage Polymer Field-Effect Transistors for Nonvolatile Memories. *Appl. Phys. Lett.* **2005**, *87*, 203509.
(20) Zaitsu, K.; Lee, S.; Ishibe, K.; Sekitani, T.; Someya, T. A Field-Cycle-Induced High-Dielectric Phase in Ferroelectric Copolymer. *J. Appl. Phys.* **2010**, *107*, 114506.
(21) Kalenbrunner, M.; Stadler, P.; Schwodiauer, R.; Hassel, A. W.; Sariciftci, N. S.; Bauer, S. Anodized Aluminum Oxide Thin Films for Room-Temperature-Processed, Flexible, Low-Voltage Organic Non-Volatile Memory Elements with Excellent Charge Retention. *Adv. Mater.* **2011**, *23*, 4892−4896.
(22) Naber, R. C. G.; Tanase, C.; Bloom, P. W. M.; Gelinck, G. H.; Marsman, A. W.; Touwslager, F. J.; Setayesh, S.; De Leeuw, D. M. High-Performance Solution-Processed Polymer Ferroelectric Field-Effect Transistors. *Nat. Mater.* **2005**, *4*, 243−248.
(23) Dao, T. T.; Matsushima, T.; Murata, H. Organic Nonvolatile Memory Transistors Based on Fullerene and an Electron-Trapping Polymer. *Org. Electron.* **2012**, *13*, 2709−2715.
(24) Hwang, S. K.; Bae, I.; Kim, R. H.; Park, C. Flexible Non-Volatile Ferroelectric Polymer Memory with Gate-Controlled Multilevel Operation. *Adv. Mater.* **2012**, *24*, 5910−5914.
(25) Hwang, S. K.; Min, S.-Y.; Bae, I.; Cho, S. M.; Kim, K. L.; Lee, T.-W.; Park, C. Non-Volatile Ferroelectric Memory with Position-Addressable Polymer Semiconducting Nanowire. *Small* **2014**, *10*, 1976−1984.
(26) Kim, S.-J.; Lee, J.-S. Flexible Organic Transistor Memory Devices. *Nano Lett.* **2010**, *10*, 2884−2890.
(27) Sekitani, T.; Zaitsu, K.; Noguchi, Y.; Ishibe, K.; Takamiya, M.; Sakurai, T.; Someya, T. Printed Nonvolatile Memory for a Sheet-Type Communication System. *IEEE Trans. Electron Devices* **2009**, *56*, 1027−1035.
(28) Chen, C.-M.; Liu, C.-M.; Wei, K.-H.; Jeng, U.; Su, C.-H. Non-Volatile Organic Field-Effect Transistor Memory Comprising Sequestered Metal Nanoparticles in a Diblock Copolymer Film. *J. Mater. Chem.* **2012**, *22*, 454−461.
(29) Hwang, S. K.; Bae, I.; Cho, S. M.; Kim, R. H.; Jung, H. J.; Park, C. High Performance Multi-Level Non-Volatile Polymer Memory with Solution-Blended Ferroelectric Polymer/High-*k* Insulators for Low Voltage Operation. *Adv. Funct. Mater.* **2013**, *23*, 5484−5493.
(30) Lee, K. H.; Lee, G.; Lee, K.; Oh, M. S.; Im, S.; Yoon, S.-M. High-Mobility Nonvolatile Memory Thin-Film Transistors with a Ferroelectric Polymer Interfacing ZnO and Pentacene Channels. *Adv. Mater.* **2009**, *21*, 4287−4291.
(31) Kang, S. J.; Bae, I.-S.; Shin, Y. J.; Park, Y. J.; Huh, J.; Park, S. M.; Kim, H. C.; Park, C. Nonvolatile Polymer Memory with Nano-confinement of Ferroelectric Crystals. *Nano Lett.* **2011**, *11*, 138−144.
(32) Kim, S. H.; Hong, K.; Xie, W.; Lee, K. H.; Zhang, S.; Lodge, T. P.; Frisbie, C. D. Electrolyte-Gated Transistors for Organic and Printed Electronics. *Adv. Mater.* **2013**, *25*, 1822−1846.
(33) Fujimoto, T.; Awaga, K. Electric-Double-Layer Field-Effect Transistors with Ionic Liquids. *Phys. Chem. Chem. Phys.* **2013**, *15*, 8983−9006.
(34) Larsson, O.; Said, E.; Berggren, M.; Crispin, X. Insulator Polarization Mechanisms in Polyelectrolyte-Gated Organic Field-Effect Transistors. *Adv. Funct. Mater.* **2009**, *19*, 3334−3341.
(35) Lee, K. H.; Lee, G.; Lee, K.; Oh, M. S.; Im, S. Flexible Low Voltage Nonvolatile Memory Transistors with Pentacene Channel and Ferroelectric Polymer. *Appl. Phys. Lett.* **2009**, *94*, 093304.
(36) Lee, K. H.; Kang, M. S.; Zhang, S.; Gu, Y.; Lodge, T. P.; Frisbie, C. D. Cut and Stick Rubbery Ion Gels as High Capacitance Gate Dielectrics. *Adv. Mater.* **2012**, *24*, 4457−4462.
(37) Baeg, K.-J.; Kim, D.; Kim, J.; Yang, B.-D.; Kang, M.; Jung, S.-W.; You, I.-K; Kim, D.-Y.; Noh, Y.-Y. High-Performance Top-Gated Organic Field-Effect Transistor Memory using Electrets for Monolithic Printed Flexible NAND Flash Memory. *Adv. Funct. Mater.* **2012**, *22*, 2915−2926.
(38) Lee, K. H.; Zhang, S.; Lodge, T. P.; Frisbie, C. D. Electrical Impedance of Spin-Coatable Ion Gel Films. *J. Phys. Chem. B* **2011**, *115*, 3315−3321.
(39) Kim, S. H.; Hong, K.; Lee, K. H.; Frisbie, C. D. Performance and Stability of Aerosol-Jet-Printed Electrolyte-Gated Transistors Based on Poly(3-hexylthiophene). *ACS Appl. Mater. Interfaces* **2013**, *5*, 6580−6585.
(40) Barker, R. E. Mobility and Conductivity of Ions in and into Polymeric Solids. *Pure Appl. Chem.* **1976**, *46*, 157−170.
(41) Li, J.; Yan, F. Solution-Processable Low-Voltage and Flexible Floating-Gate Memories Based on an n-Type Polymer Semiconductor and High-k Polymer Gate Dielectrics. *ACS Appl. Mater. Interfaces* **2014**, *6*, 12815−12820.
(42) Park, Y. J.; Kang, S. J.; Park, C.; Lotz, B.; Thierry, A.; Kim, K. J.; Huh, J. Molecular and Crystalline Microstructure of Ferroelectric Poly(vinylidene fluoride-co-trifluoroethylene) Ultrathin Films on Bare and Self-Assembled Monolayer-Modified Au Substrates. *Macromolecules* **2008**, *41*, 109−119.
(43) Jung, H. J.; Chang, J.; Park, Y. J.; Kang, S. J.; Lotz, B.; Huh, J.; Park, C. Shear-Induced Ordering of Ferroelectric Crystals in Spin-Coated Thin Poly(vinylidene fluoride-co-trifluoroethylene) Films. *Macromolecules* **2009**, *42*, 4148−4154.
(44) Sirringhaus, H.; Brown, P. J.; Friend, R. H.; Nielsen, M. M.; Bechgaard, K.; Langeveld-Voss, B. M. W.; Spiering, A. J. H.; Janssen, R.

A. J.; Meijer, E. W.; Herwig, P.; De Leeuw, D. M. Two-Dimensional Charge Transport in Self-Organized, High-Mobility Conjugated Polymers. *Nature* **1999**, *401*, 685−688.